TIPTEKNO'18
TIP TEKNOLOJİLERİ KONGRESİ
8-10 Kasım 2018 / Gazi Magosa / KKTC
İZMİR KÂTİP ÇELEBİ ÜNİVERSİTESİ
BİYOMEDİKAL MÜHENDİSLİĞİ BÖLÜMÜ

Changes of Visual Networks at Resting State in Children with Attention Deficit Hyperactivity Disorder

Şerife Gengeç Benli[1], Semra İçer[1], Sevgi Özmen[2]

[1]Department of Biomedical Engineering, Faculty of Engineering, Erciyes University, Turkey
serifegengec@erciyes.edu.tr, ksemra@erciyes.edu.tr
[2]Department of Child and Adolescent Mental Health and Diseases, Faculty of Medicine, Erciyes University, Turkey
drsevgiozmen@gmail.com

***Abstract*—Attention deficit hyperactivity disorder (ADHD) characterized by hyperactive, impulsive, and/or inattentive behaviors is one of the most common childhood disorder. ADHD has frequently been associated with changes in resting-state functional connectivity. In last two decades, blood oxygen level dependent (BOLD) fMRI has become an important neuroscientific tool because of ability to image brain function. In this current study, we examined functional connectivity within various visual networks occuring at resting state in children with and without ADHD. It is performed by independent component analysis within group analysis. We found four independent components (ICs) which are included of visual networks. Significant differences were obtained in activation regions of visual networks. The study aimed to contribute to the characterization of ADHD by identifying the specific changes that occur in the visual networks which include of resting state networks.**

Keywords — ADHD; resting state; visual networks.

I. INTRODUCTION

Attention deficit hyperactivity disorder (ADHD) characterized by hyperactive, impulsive, and/or inattentive behaviors is one of the most common developmentally childhood disorder, affects 5% or more of school-aged children [1, 2]. ADHD has frequently been associated with changes in resting-state functional connectivity. Especially occuring changes of resting state networks in ADHD help to investigate neurobiological underpinning.

Functional magnetic resonance imaging (fMRI) is high spatial resolution brain mapping that shows MR signal changes due to tissue oxygenation in the brain at resting state (rs) or in a busy task. As well as, this functional imaging technique used to diagnose many neurological and psychiatric disorders like ADHD.

Resting state studies suggest that there are many advantages to examine functional organization of brain networks, according to task-based studies [3].

First, while spontaneous activity accounts a large majority of brain activity, on the other side increases of neural metabolism are usually small in the task (<5%) [4].To fully understand the brain function, it is important to assess spontaneous activity of the brain during rest [5]. Secondly, while resting state studies are largely free of potentially confounding effects for healthy and patients, it is difficult to achieve an equal level of performance for the patient and control group in a task [6, 7]. Finally, resting state studies lead to less activity than task-based fMRI studies that require response with motor activity [8]. The researches of rs-fMRI have yielded heterogeneous and inconsistent results. In literature default mode network (DMN) connectivity changes were examined commonly. Decreased [9] or increased [10] functional connectivity in DMN has been reported. Brain abnormalities have been found not only in the DMN but also in other brain regions including the parietal, temporal, visual, attention, central executive, cerebellar network in ADHD subjects. Cai et al. examined salience network, left central executive network, right central executive network, defult mode network. They also determined network dysregulation measures can differentiate children with ADHD from control subjects [11]. Choi et al. identified as different visual networks of three of the twelve resting networks. They calculated spatial correlation coefficients between corresponding resting state networks (RSNs) from each group from RSN1 to RSN12. They reported that spatial patterns of RSNs were consistent [12]. While there are many different RSNs studies at resting state related with ADHD in the literature, visual network studies are not sufficient and detailed.

The purpose of this study was to determine the changes in the connectivity of various visual networks in children with ADHD according to typically development (TD) children at resting state. It is thought that the acquired findings will contribute to the characterization of ADHD.

978-1-5386-6852-8/18/$31.00 ©2018 IEEE

II. PARTICIPANTS and DATA ACQUISITION

2.1. Participants

This study was approved by the local Ethics Committee (Decision no: 2013/689). A total of fourty right-handed children, 20 with a diagnosis of ADHD and 20 matched typically developing (TD) peers-aged 9 through 16 years included in the study. The mean age was 11.8±2.29 years for the ADHD group and 13 ± 1.78 years for the TD group. Here, magnetic resonance imaging data from 4 female and 16 male in ADHD group, 10 male and 10 female in control group were acquired.
ADHD groups occured with the children who diagnosed with ADHD for the first time and they were medication-naïve. The children in control group had no history of psychiatric disorder. The diagnosis of ADHD was made, based on the DSM-IV Based Behavior Disorders Screening and Ratings Scale and Conners Rating Scale by an expert pediatric psychiatrist. Subjects with intelligent quotient score (IQ) of above 85 were selected according Wechsler Abbreviated Scale of Intelligence.

2.2. Structural data acquisition

Imaging was performed using a 1.5 Tesla clinical scanner (Magnetom Aera, Siemens Healthcare, Erlangen, Germany) which included a 20-channel head coil at the Radiology Department of Erciyes University Pediatric Hospital. Structural image data were acquired with T1-weighted magnetization prepared rapid acquisition gradient-echo (MPRAGE) sequence. Implemented scan parameters are sagittal orientation, echo time (TE)=2.670 ms, repetition time (TR)=1900 ms, 256×256 matrix, isotropic resolution=1.3 mm and total scan time = 4 min 18 sec for 192 slices respectively.

2.3. Functional data acquisition

BOLD-weighted functional image data were acquired using T2*-weighted echo-planar imaging sequence with the following imaging parameters: TR= 2800 ms, TE=25ms, flip angle = 90°, field of view =192 mm, 36 slices covering the whole brain, slice thickness = 3 mm, in-plane resolution =2×2 mm. Resting state data was collected for 9 min 44 s resulting in 205 volumes of BOLD fMRI data per participant. Participants were instructed during scanning to lay still with their eyes closed, remain awake and relaxed, and to let their thoughts change during scanning.

III. METHOD

3.1. Preprocessing

Data were preprocessed using the Statistical Parametric Mapping software package, SPM8. The first five BOLD scans were discarded for image stabilization. The remaining 200 images were spatially realigned to the first volume as a reference volume using rigid-body translation and rotation. For this purpose, six parameters (x, y, z and pitch, yaw, roll) were obtained by correction for rigid body head motion. After that fMRI data were eliminated based on translation parameters >0.3 mm and rotation parameters >0.3 degrees. Each participant's structural images were coregistered with functional images. Spatial smoothing using a Gaussian kernel of full-width at half-maximum 6 mm was performed to reduce noise.

3.2. Independent component analysis

Independent component analysis (ICA) is a technique which decomposes a two-dimensional (time×voxels) data matrix into a set of time-courses and related spatial maps [13]. ICA is based on the separation of the measured data set into independent statistically independent components that are as independent as possible.
The ICA is often used to find back the original signals from the measured signals as a mixture of signals from different sources. If the measured signal and source signal are indicated by 'x' and 's' respectively, the relationship between measured signal and the source signal can be expressed as equation 1.

$$x = As \tag{1}$$

ICA produces specific brain activation maps of a group or individual without prior assumption of time and pattern knowledge of response markers dependent on blood oxygenation level. In this way, functional interrelated brain regions and other noise-related signals can be separated into temporal and spatial components.
In this study, Group ICA was performed using the GIFT toolbox The Infomax group ICA algorithm was repeated 50 times in ICASSO for 30 Independent Components. Out of the 30 components obtained, we characterized 4 components belonging to visual networks which included of resting state networks. For visualization, maps were thresholded by z-value $(|z| \geq 3)$.

IV. RESULTS

In this study, we have examined four independent components (ICs) belonging to visual networks. Here, IC-14 and IC-18 represent medial visual network. Also IC-20 and IC-22 represent lateral visual network and extrastriate visual network respectively. These networks were identified as their coordinates and literature.
We performed within group analysis both in children with and without ADHD. The threshold has been selected $(|z| \geq 3)$ for presenting of resting state networks as spatial maps. One-sample t test was performed with a statistical significance level of $p < 0.05$ (FDR corrected) both two groups.
IC-14, IC-18, IC-20 and IC-22 were evaluated according Talairach table results given in Table 1. Decreases and increases in functional activity of both two groups were determined with this table.
IC-14 spatial map is given in (Fig. 1). Evaluated IC-14, children with ADHD revealed decreased functional activity in bilateral lingual gyrus, bilateral sub-gyral and right cuneus and increased functional connectivity in the

left cuneus, bilateral middle occipital gyrus and bilateral inferior occipital gyrus compared with TD children.

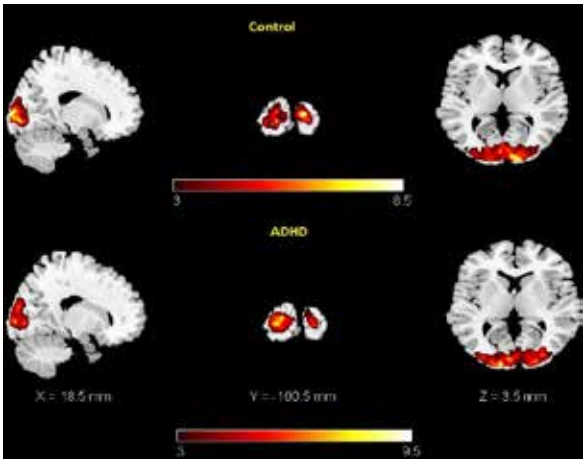

Fig. 1. IC-14: Medial visual network

IC-18 spatial map is given in (Fig. 2). Evaluated IC-18, children with ADHD revealed decreased functional activity in the bilateral posterior cingulate, bilateral lingual gyrus, left culmen, left precuneus, left fusiform gyrus, left sub-gyral, left middle occipital and bilateral extra-nuclear compared with TD children. In addition to increased functional activity was shown in bilateral cuneus, right culmen, right precuneus, rigt fusiform gyrus, right sub-gyral, right declive, right middle temporal gyrus, right parahippocampal gyrus.

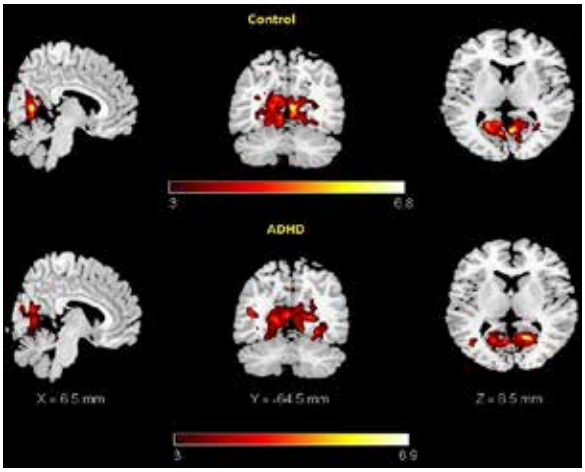

Fig. 2. IC-18: Medial visual network

IC-20 spatial map is given in (Fig. 3). According IC-20, children with ADHD revealed decreased functional activity in the left declive, left culmen left cuneus, left middle frontal gyrus as well as increased functional connectivity in right middle occipital gyrus, right inferior temporal gyrus, left superior temporal gyrus, left inferior occipital gyrus, right lingual gyrus and right cuneus.

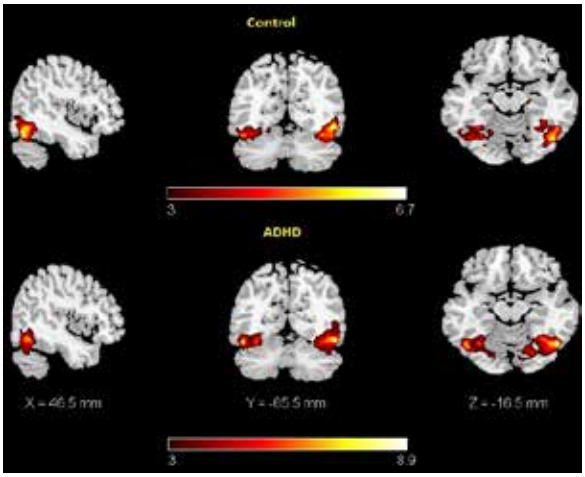

Fig. 3. IC-20: Lateral visual network

IC-22 spatial map is given in (Fig. 4). According IC-22, children with ADHD revealed decreased functional activity in bilateral cuneus, left sub-gyral, left middle occipital gyrus as well as increased functional connectivity in the bilateral precunues, bilateral superior parietal lobule, right sub-gyral, right middle occipital gyrus, right middle temporal gyrus, right superior occipital gyrus.

V. DISCUSSION

In this study, we found significant differences in medial visual networks, lateral visual network and extrastriate visual network between children with and without ADHD at resting state. The majority of ADHD studies involving the visual network are based on task and award process. Resting state studies can be considered to give more reliable and consistent results because of stabilization in sense and thought. Thus resting state studies increasingly gain importance. It may be very important to understand and evaluate to ADHD given changes related visual networks between ADHD and control in this study.

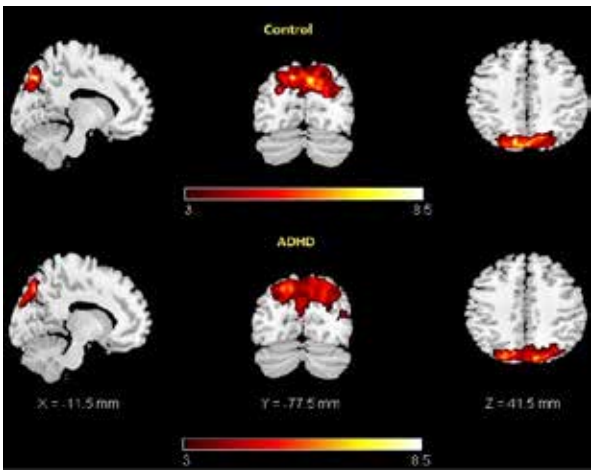

Fig. 4. IC-22: Extrastriate visual network

RERERENCES

[1] Bos, D.J., Oranje, B., Achterbeg M., et al. "Structural and functional connectivity in children and adolescents with and without attention deficit hyperactivity disorder", J. Child Psychol. Psychiatry., Vol. 58, No. 7, pp. 810–818, 2017.

[2] Malhotra, S., Bhatia, N.K., Kumar P., et al. "The potential role of infections in attention deficit hyperactivity disorder", Delhi Psychiatry Journal, Vol. 14 No.2, pp. 361-367, 2011.

[3] Pearlson, G.D. and Calhoun V.D. "Convergent approaches for defining functional imaging endophenotypes in schizophrenia", Front Hum Neurosci. Vol.3, No.37, 2009.

[4] Raichle, M.E. and Mintun, M.A. "Brain work and brain imaging", Annu Rev Neurosci. Vol.29, pp, 449–476, 2006.

[5] Raichle M.E., "Two views of brain function", Trends in cognitive sciences, Vol. 14 No. 4, pp. 180–190, 2010.

[6] Fox, M.D. and Raichle, M.E. "Spontaneous fluctuations in brain activity observed with functional magnetic resonance imaging", Nat. Rev. Neurosci., Vol. 8, No. 9, pp. 700–711, 2007.

[7] Greicius, M. "Resting-state functional connectivity in neuropsychiatric disorders", Curr. Opin. Neurol., Vol. 21, No. 4 pp. 424–430, 2008.

[8] Rosazza, C., Minati, L. "Resting-state brain networks: literature review and clinical applications", Neurol Sci., Vol. 32, No.5, pp.773–785, 2011.

[9] Qiu, M., Ye, Z., Li, Q., et al. "Changes of brain structure and function in ADHD children", Brain Topography, Vol. 24, pp. 243-252, 2011.

[10] Barber, A.D., Jacobson, L.A., Wexler, J.L., et al. "Connectivity supporting attention in children with attention deficit hyperactivity disorder", Neuroimage Clin, Vol. 7, pp. 68-81, 2015.

[11] Cai, W., Chen, T., Szegletes, L., et al. "Aberrant cross-brain network interaction in children with attention-deficit/hyperactivity disorder and its relation to attention deficits: A multisite and cross-site replication study", Biol Psychiatry, Vol. 81, No. 1, pp. 86, 2017.

[12] Choi, J., Jeong, B., Lee, S.W., Go H.J. "Aberrant development of functional connectivity among resting state-related functional networks in medication-naïve ADHD children", PLoS One, Vol. 8. No. 12, pp. e83516, 2013.

[13] Beckmann, C.F., DeLuca M., Devlin, J.T., Smith S.M. "Investigations into resting-state connectivity using independent component analysis", Philos Trans R Soc Lond B Biol Sci., Vol. 360, No. 1457, pp. 1001-1013, 2005.

Table 1. Regions which are related with visual networks activated in controls and ADHD at resting state

Area	Brodmann Area	L/R volume (cc)	L/R: Max Z(x, y, z)
IC-14: Medial visual network			
Control			
Cuneus	17, 18, 19, 23, 30	6.2/6.5	7.1 (-12, -97, 0)/8.4 (18, -97, 9)
Middle cccipital gyrus	18, 19	3.3/4.2	5.2 (-22, -89, 15)/8.1 (10, -91, 14)
Lingual gyrus	17, 18	3.0/3.3	5.8 (-26, -97, -4)/8.1 (20, -87, 1)
Sub-gyral	*	0.6/0.8	5.7 (-32, -87, -1)/7.7 (26, -87, -1)
Inferior occipital gyrus	17, 18, 19	0.6/0.4	5.4 (-24, -96, -7)/3.8 (40, -82, -1)
Lateral ventricle	*	0.1/0.0	3.4 (-32, -39, 2)/ns
Inferior temporal gyrus	*	0.0/0.1	ns/3.4 (50, -72, -1)
ADHD			
Middle occipital gyrus	18, 19	4.0/5.3	10.0 (-32, -85, 3)/6.6 (24, -93, 6)
Cuneus	17, 18, 19, 30	6.3/5.7	8.5 (-20, -97, 3)/7.4 (20, -95, 5)
Lingual gyrus	17, 18	2.9/2.0	5.3 (-14, -89, 3)/6.9 (20, -81, 4)
Sub-gyral	*	0.3/0.4	6.0 (-26, -89, 1)/4.4 (26, -91, 0)
Inferior occipital gyrus	17, 18, 19	1.0/0.5	5.8 (-38, -87, -1)/3.7 (36, -89, -1)
Middle temporal gyrus	21, 22	0.1/0.3	3.2 (-57, -47, -6)/4.6 (61, -37, 0)
Precuneus	31	0.0/0.1	ns/3.7 (24, -80, 26)
Postcentral gyrus	*	0.1/0.0	3.3 (-44, -24, 55)/ns
IC-18: Medial visual network			
Control			
Cuneus	18, 23, 30	1.0/1.0	4.5 (-6, -68, 7)/6.8 (6, -62, 9)
Posterior cingulate	23, 29, 30, 31	2.9/2.6	6.4 (-4, -66, 11)/5.8 (10, -60, 10)
Lingual gyrus	18, 19	2.8/3.1	6.2 (-12, -54, 3)/6.3 (22, -68, -5)
Culmen	*	1.1/0.3	5.3 (-6, -61, -7)/3.8 (8, -66, -3)
Precuneus	31	1.2/0.8	5.2 (-10, -61, 18)/4.6 (4, -69, 24)
Fusiform gyrus	19	0.4/0.3	4.6 (-20, -63, -9)/3.7 (26, -57, -7)
Sub-gyral	*	1.2/1.3	4.5 (-14, -59, 20)/4.4 (26, -70, -2)
Parahippocampal gyrus	19, 30	0.4/0.0	4.1 (-16, -50, 4)/ns
Middle occipital gyrus	*	0.3/0.1	4.0 (-28, -62, 5)/3.4 (28, -56, 5)
Middle temporal gyrus	*	0.1/0.0	3.9 (-32, -61, 18)/ns
Extra-nuclear	*	0.4/0.4	3.7 (-20, -54, 12)/3.8 (22, -54, 12)
Superior frontal gyrus	*	0.1/0.0	3.7 (0, 14, 51)/ns
Declive	*	0.2/0.1	3.5 (-30, -53, -11)/3.4 (8, -74, -11)
ADHD			
Posterior cingulate	23, 29, 30, 31	1.7/2.4	5.4 (-4, -64, 11)/7.1 (16, -58, 10)
Cuneus	7, 17, 18, 23, 30	2.4/1.8	6.4 (0, -75, 20)/5.2 (2, -79, 22)
Fusiform gyrus	19, 37	0.2/0.4	3.7 (-20, -66, -7)/5.4 (26, -53, -9)
Lingual gyrus	18, 19	2.5/2.2	5.1 (-16, -62, 5)/5.2 (8, -66, 5)
Extra-nuclear	*	0.1/0.2	3.4 (-20, -54, 10)/5.1 (24, -60, 9)
Middle temporal gyrus	19, 39	0.4/0.1	5.0 (-42, -64, 11)/3.6 (32, -67, 20)
Culmen	*	0.5/0.7	4.0 (-18, -57, -7)/4.9 (10, -56, -1)
Parahippocampal gyrus	19, 30	0.2/0.3	3.4 (-22, -57, -6)/4.6 (28, -57, -6)
Precuneus	23, 31	0.9/1.0	4.5 (-8, -70, 27)/4.1 (6, -67, 20)
Sub-gyral	*	0.8/1.7	4.1 (-38, -62, 10)/4.2 (24, -65, 24)
Lateral ventricle	*	0.1/0.2	4.1 (-26, -48, 6)/3.6 (28, -64, 7)
Superior temporal gyrus	39	0.1/0.0	3.9 (-46, -61, 18)/ns
Declive	*	0.3/0.4	3.7 (-28, -65, -12)/3.8 (26, -63, -12)
Middle occipital gyrus	*	0.2/0.1	3.5 (-42, -68, 9)/3.1 (28, -58, 5)
IC-20: Lateral visual network			
Control			
Declive	*	2.0/2.3	7.0 (-46, -55, -19)/5.8 (44, -69, -15)
Middle occipital gyrus	19, 37	0.4/1.8	4.4 (-40, -68, -10)/6.2 (50, -64, -7)
Fusiform gyrus	19, 37	1.9/2.2	5.4 (-50, -57, -17)/6.0 (46, -71, -12)
Inferior temporal gyrus	20, 21, 37	0.1/0.9	4.2 (-51, -57, -11)/5.4 (57, -61, -9)
Middle temporal gyrus	37	0.0/0.3	ns/5.3 (53, -59, -9)
Sub-gyral	*	0.3/0.9	3.8 (-42, -65, -9)/5.1 (48, -63, -10)
Parahippocampal gyrus	30, 36	0.0/0.3	ns/4.4 (16, -43, 2)
Culmen	*	0.3/0.3	4.1 (-4, -40, -22)/3.8 (34, -48, -19)

Superior temporal gyrus	22	0.0/0.1	ns/4.1 (61, 4, 2)
Medial frontal gyrus	*	0.0/0.1	ns/3.9 (2, -9, 48)
Inferior occipital gyrus	19	0.0/0.1	ns/3.8 (40, -74, -6)
Lingual gyrus	*	0.1/0.0	3.7 (-24, -59, -5)/ns
Cuneus	19	0.1/0.0	3.3 (-14, -88, 34)/ns
Inferior frontal gyrus	*	0.0/0.1	ns/3.3 (61, 12, 12)
Posterior cingulate	*	0.1/0.0	3.3 (-6, -42, 8)/ns
Precentral gyrus	4	0.0/0.3	ns/3.2 (50, -3, 11)
Extra-nuclear	*	0.1/0.1	3.1 (-16, 0, -7)/3.1 (8, -31, 2)
Middle frontal gyrus	*	0.1/0.0	3.0 (-36, 18, 43)/ns
ADHD			
Middle occipital gyrus	19, 37	1.0/1.5	5.2 (-46, -68, -8)/8.6 (51, -63, -10)
Fusiform gyrus	19, 37	1.9/3.3	7.8 (-48, -63, -12)/6.4 (42, -61, -12)
Declive	*	1.6/3.5	5.6 (-34, -65, -14)/6.2 (24, -74, -13)
Sub-gyral	*	0.6/0.9	5.2 (-48, -61, -9)/6.2 (44, -65, -10)
Lingual gyrus	18	0.2/0.8	3.6 (-20, -76, -10)/5.0 (24, -74, -10)
Inferior temporal gyrus	19, 21	0.1/0.3	3.0 (-63, -9, -18)/5.0 (51, -60, -2)
Culmen	*	0.1/0.4	3.0 (-38, -55, -19)/4.8 (42, -44, -20)
Middle temporal gyrus	21, 37	0.0/0.8	ns/4.4 (55, -58, 0)
Superior temporal gyrus	38	0.1/0.1	3.1 (-48, 12, -26)/3.8 (69, -15, 8)
Inferior occipital gyrus	18, 19	0.1/0.1	3.6 (-34, -82, -14)/3.0 (42, -76, -3)
Transverse temporal gyrus	*	0.0/0.1	ns/3.6 (67, -11, 10)
Posterior cingulate	29, 30	0.1/0.1	3.5 (-6, -52, 6)/3.1 (4, -54, 10)
Cuneus	19	0.0/0.1	ns/3.3 (10, -88, 30)
Middle frontal gyrus	*	0.0/0.1	ns/3.2 (48, 25, 28)
Tuber	*	0.0/0.2	ns/3.2 (44, -65, -24)
Precentral gyrus	*	0.0/0.1	ns/3.1 (55, 2, 11)
Precuneus	*	0.0/0.1	ns/3.1 (2, -46, 56)
IC-22: Exstrastriate visual network			
Control			
Precuneus	7, 19, 31	5.3/6.6	8.9 (-12, -74, 42)/7.6 (18, -68, 40)
Cuneus	7, 18, 19	4.1/4.2	6.8 (-18, -88, 32)/6.9 (2, -82, 26)
Sub-gyral	*	0.5/1.0	6.6 (-26, -72, 29)/5.4 (24, -75, 24)
Angular gyrus	39	0.0/0.2	ns/5.7 (38, -76, 30)
Superior parietal lobule	7	0.3/0.6	4.8 (-24, -72, 44)/5.1 (18, -69, 53)
Middle occipital gyrus	18, 19	0.3/0.3	4.0 (-40, -85, 10)/4.1 (30, -79, 21)
Middle temporal gyrus	19, 39	0.1/0.3	3.3 (-36, -81, 19)/3.6 (34, -77, 20)
Superior occipital gyrus	19	0.1/0.3	3.4 (-28, -80, 26)/3.4 (34, -78, 28)
Inferior parietal lobule	*	0.0/0.1	ns/3.4 (42, -58, 42)
ADHD			
Precuneus	7, 19, 31	5.9/8.2	8.6 (-18, -78, 37)/7.6 (14, -78, 41)
Cuneus	7, 18, 19, 23	4.0/3.6	6.1 (-18, -82, 37)/7.2 (16, -82, 35)
Superior occipital gyrus	19	0.1/0.5	4.4 (-30, -88, 25)/5.4 (40, -80, 28)
Middle occipital gyrus	19	0.2/0.6	5.3 (-30, -88, 21)/4.4 (30, -82, 21)
Superior parietal lobule	7	0.5/0.9	4.3 (-24, -73, 46)/5.3 (30, -75, 46)
Middle temporal gyrus	*	0.1/0.4	3.2 (-38, -75, 20)/4.8 (42, -71, 16)
Sub-gyral	*	0.1/1.1	3.7 (-28, -74, 33)/4.4 (30, -76, 33)
Angular gyrus	39	0.0/0.1	ns/3.8 (38, -76, 31)

*Voxels above threshold were converted from MNI to Talairach coordinates and entered into a database to provide anatomic and functional labels for the left (L) and right (R) hemispheres. The volume of activated voxels in each area is provided in cubic centimeter (cc). ns: not significant